Materials Science & Engineering C 92 (2018) 416–423

Contents lists available at ScienceDirect

Materials Science & Engineering C

journal homepage: www.elsevier.com/locate/msec

# Carbon nanoparticles suspension injection for the delivery of doxorubicin: Comparable efficacy and reduced toxicity

Yuanfang Huang[a,b], Ping Xie[a,*], Sheng-Tao Yang[c,*], Xuemei Zhang[b], Guangfu Zeng[b], Qian Xin[b], Xiao-Hai Tang[b,*]

[a] State Key Laboratory of Oral Diseases, West China College of Stomatology, Sichuan University, Chengdu 610041, China
[b] Chongqing Lummy Pharmaceutical Co., Ltd., Chongqing 401123, China
[c] College of Chemistry and Environment Protection Engineering, Southwest Minzu University, Chengdu 610041, China

ARTICLE INFO

*Keywords:*
Carbon nanoparticles suspension injection
Doxorubicin
Toxicity
Drug delivery
Tumor

ABSTRACT

Drug delivery systems for doxorubicin (DOX) have attracted tremendous interest nowadays for the improved efficacy and/or reduced toxicity. Due to the aromatic structures and hydrophobic domains, carbon nanoparticle suspension injection (CNSI), a clinical applied reagent for lymph node mapping, strongly adsorbs DOX and holds great potential in cancer therapy. Herein, we evaluated the therapeutic effects of CNSI-DOX to establish its delivery applications for cancer drugs. CNSI adsorbed DOX from solution quickly after the mixing, and the release of DOX from CNSI followed a pH-dependent way. CNSI-DOX and free DOX had nearly identical inhibitive effects on cancer cells, while the vehicle CNSI was nontoxic. CNSI-DOX largely prolonged the life span of ascites tumor bearing mice after the intraperitoneally injection and the ascites weights showed significant decreases. CNSI-DOX also inhibited the growth of subcutaneous xenografts following the same administration route. The therapeutic efficacy of CNSI-DOX was similar to that of free DOX in ascites tumor model, but slightly lower in subcutaneous xenografts model. The advantage of using CNSI was majorly reflected by the reduced toxicity of DOX according to the bodyweight changes, serum biochemical indicators and histopathological observations. The $LD_{50}$ (median lethal dose) value of CNSI-DOX was 43.8 mg/kg bodyweight, nearly three times of that of free DOX (15.2 mg/kg bodyweight). Our results suggested that CNSI might be used for DOX delivery through "off label" use to benefit the patients immediately.

## 1. Introduction

Doxorubicin (DOX) is an anthracycline anticancer drug for the therapy of both solid and hematologic malignancies [1,2]. However, its clinical use is largely limited by its bone marrow toxicity, gastrointestinal toxicity, and cardiotoxicity [3–5]. Therefore, the major issue in DOX therapy is to reduce its toxicity and maintain its efficacy simultaneously. Typically, there are two main strategies for this purpose. First, the antioxidants could eliminate the reactive radicals generating during the DOX treatment and protect the patients from cardiotoxicity [6–8]. Second, the drug delivery system (DDS) could enhance the tumor uptake and reduce the non-specific accumulation of DOX to reduce its toxicity and improve its efficacy [9–12]. For this pathway, diverse vehicles were reported worldwide, such as liposomes [13], polymer carriers [14], and inorganic nanomaterials [15].

In recent decades, carbon nanomaterials have attracted great interest in DOX therapy for both the anti-oxidation and the delivery. For instance, fullerenol was found to be good antioxidant and protected the body from the DOX toxicity [16]. On the other hand, DOX has large aromatic rings in the structure and is partially hydrophobic, which strongly binds to carbon nanomaterials through π-π interaction and hydrophobic interaction [17]. Another merit of using carbon nanomaterials as delivery vehicles could be that DOX shows pH-dependent release on carbon nanomaterials [17]. More DOX molecules detach from carbon surface at acidic pH values, thus would hopefully become free forms at the tumor site. Many carbon nanomaterials have been used in delivering DOX, including carbon nanotubes (CNTs) [18], graphene [19], carbon dots [20], and so on. For example, Wang et al. coated CNTs with gold and built a target delivery system for DOX [21]. The gold coated CNTs delivered DOX into cancer cells and could be used for photothermal therapy simultaneously. He et al. used graphene oxide for the pH-sensitive delivery of short hairpin RNA and DOX [22]. The DDS silenced the multidrug resistant gene expression and increased chemotherapy efficacy of DOX. Despite the encouraging achievements,

* Corresponding authors.
*E-mail addresses:* xieping318@aliyun.com (P. Xie), yangst@pku.edu.cn (S.-T. Yang), pharmmateceo@aliyun.com (X.-H. Tang).

https://doi.org/10.1016/j.msec.2018.07.012
Received 2 January 2018; Received in revised form 27 June 2018; Accepted 3 July 2018
Available online 04 July 2018
0928-4931/ 

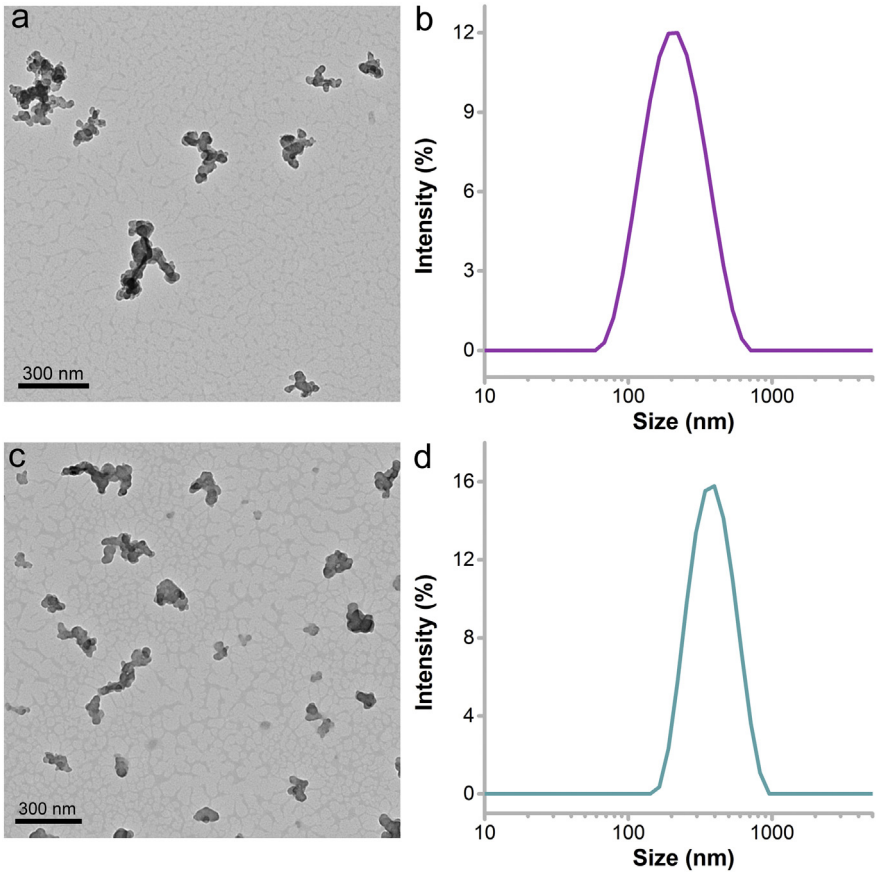


**Fig. 1.** TEM images (a, c) and DLS data (b, d) of CNSI (a, b) and CNSI-DOX (c, d).

these carbon nanomaterials have not been applied in clinical treatments, because they have to pass through phases of clinical trials before the approval.

Among the novel carbon nanomaterials, carbon nanoparticle suspension injection (CNSI) is the only commercialized and clinically applied one [23]. CNSI is capable in staining the tumor drainage lymph node black after the intratumoral injection. Successful demonstrations were achieved on advanced gastric cancer [24], breast cancer [25] and papillary thyroid carcinoma [26]. Separately, CNSI does not stain the parathyroid gland during the thyroid carcinoma surgery, so the risk of false resection could be largely reduced with the injection of CNSI [27]. In addition, CNSI is of very low toxicity upon exposure based on animal experiments and the clinical observations [28]. Each year, over 100, 000 patients received CNSI injection during the oncological surgery for lymphatic mapping and/or the parathyroid gland distinguishing [28]. Therefore, unlike other carbon nanomaterials, if CNSI could be used for drug delivery, it would be immediately accessible for cancer patients through 'off label' use.

Very recently, CNSI was found to adsorb drugs effectively and showed competitive performance on cellular level [29,30]. We reported that CNSI could selectively adsorb DOX and epirubicin (EPI), rather than paclitaxel, *cis*-platinum and 5-fluorouracil [29]. CNSI delivered DOX and EPI showed nearly the same inhibition rates of cancer cells as their free forms. Separately, Yang et al. mixed CNSI and EPI for the regional injection to tumor [30]. CNSI increased the lymphatic uptake of EPI and reduced the blood concentration of EPI, thus resulting in a slow release to lymph nodes. CNSI delivered EPI and free EPI had similar therapeutic effect as indicated by the same apoptosis levels of lymph nodes. Therefore, CNSI holds great promise in drug delivery and the tumor inhibition of CNSI delivered drugs should be measured to validate the concept.

Herein, we evaluated the therapeutic efficacy and toxicity of CNSI delivered DOX (CNSI-DOX) in tumor bearing mice to show the potential of CNSI in drug delivery. The adsorption and desorption of DOX on CNSI was studied in solution. The cell viabilities of cancer cells were assayed to show the in vitro efficacies of CNSI-DOX in comparison with free DOX. The in vivo evaluations were performed on xenograft models that received injections of H22 cells both intraperitoneally and subcutaneously. The survival rates, ascites weights, tumor volumes and tumor weights were monitored. The toxicity of CNSI-DOX and free DOX was compared by measuring the body weights, serum biochemistry, histopathology and $LD_{50}$ (median lethal dose) values. The implication of CNSI for cancer drug delivery is discussed.

## 2. Experimental

### 2.1. Materials

CNSI was provided by Chongqing Lummy Pharmaceutical Co. Ltd. (Chongqing, China). The preparation protocol of CNSI was briefly described as follows. Polyvinyl pyrrolidone (PVP) was sonicated in saline to obtain 20 mg/mL solution. The carbon ash was added to PVP solution at the concentration of 50 mg/mL and submitted to homogenization at 25,000 rpm for 5 min. The as-obtained black dispersion of carbon nanoparticles was CNSI.

Doxorubicin hydrochloride was purchased from Biotang Inc. (Waltham, MA, USA). Saline and sodium citrate were purchased from Sichuan Kelong Co., Ltd. (Chengdu, China). DMEM medium with high glucose, penicillin & streptomycin solution, 0.25% trypsin solution, and PBS buffer solution was brought from Thermo Fisher Scientific Inc. (Waltham, MA, USA). Fetal bovine serum (FBS) was purchased from Gibco Co. (Grand Island, NY, USA). CCK8 kits were purchased from Dojindo Laboratories (Mashikimachi, Japan). Murine H22 hepatoma cells, Hela cells, SMMC-7721cells and MCF-7cells were provided by

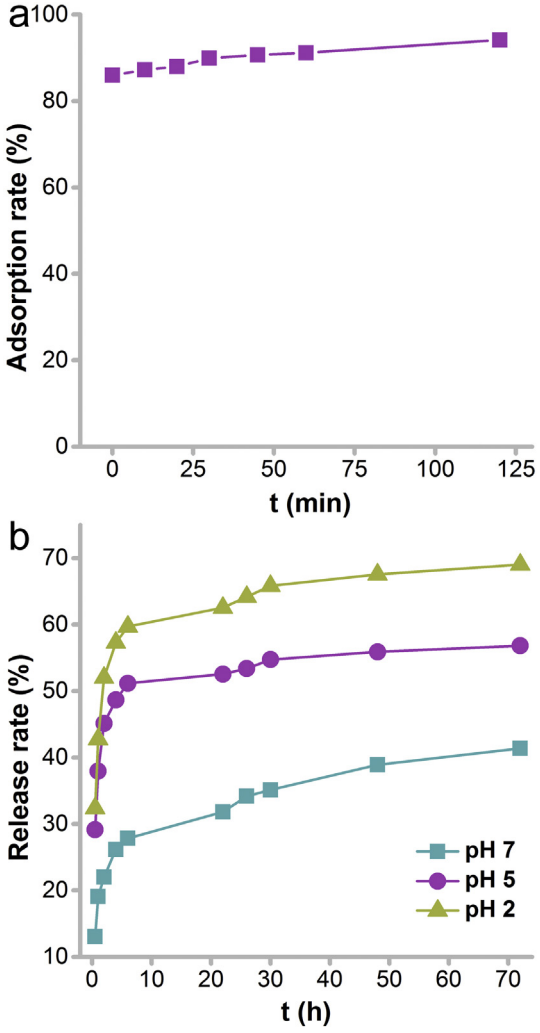


**Fig. 2.** Adsorption (a) and release (b) of DOX on CNSI as a function of time.

State Key Laboratory of Biotherapy of Sichuan University (Chengdu, China). KM mice were bought from Chengdu Dossy Experimental Animal Co. Ltd. (Chengdu, China). All other chemicals were of analytical grade.

### 2.2. Adsorption and release of DOX on CNSI

For the adsorption evaluation, DOX (2 mg/mL) and CNSI (10 mg/mL) were 1:1 (v/v) mixed and sonicated for 5 min. The mixture was shaken at 37 °C and 120 rpm for 0–120 min before the adsorption rate determination. At the designed time intervals, 2 mL of the mixture was added into a Millipore tube (Amicon ultra-4 with filter size of 50 kD) and filtered by the centrifugation of 4000 rpm for 10 min. The free DOX concentration in filtrate was measured by high performance liquid chromatography (HPLC) as described in our previous report, and the adsorption rate was calculated [29]. In addition, the particles sizes of CNSI and CNSI-DOX were analysed by a Malvern particle size analyser (Zerasizer Nano ZS90, Malvern Instruments, UK). Both CNSI and CNSI-DOX were checked under transmission electron microscope (TEM), too.

For the release evaluation, CNSI-DOX suspension was transferred into a dialysis bag (molecular mass cut-off of 50 kD) and placed into100 mL of saline (pH 7.0), PBS (pH 5.0) or PBS (pH 2.0), separately. The release was performed at 37 °C and 120 rpm. The drug concentrations in the media were measured by HPLC for release rate calculation.

### 2.3. In vitro evaluations

Hela cells, SMMC-7721 cells and MCF-7 cells were maintained at 37 °C in a humidified atmosphere with 5% $CO_2$ and the DMEM cell culture medium was supplemented with 10% FBS and 1% penicillin and streptomycin. Cells were cultured in 96-well plates with the cell density of $5 \times 10^3$ cells per well. After culturing for 24 h, the various concentrations of CNSI-DOX were added to the cells. DOX, CNSI and drug-free DMEM medium were taken as the reference groups. After 48 h incubation, FBS-free DMEM medium was used to substitute the culture medium and then added with 1/10 (v/v) of CCK-8 reagent. After an incubation for another 2 h, the absorbance was measured at 450 nm using a microplate reader (Multiskan FC, Thermo Fisher Scientific Co., USA) for viability calculation.

### 2.4. Antitumor efficacy evaluations in vivo

The animal experiments were approved by the Animal Centre of Southwest Minzu University and performed in accordance with the Animal Care and Use Program Guidelines of the Sichuan Province, China. The mice were raised in plastic cages (5 mice/cage) on a 12-h light/dark cycle with free access to food and water. The ascites tumor model was established by inoculating intraperitoneally with hepatocellular carcinoma H22 cells ($2 \times 10^6$ cells per mouse). Three days later, when the abdominal girth showed significantly increases, the mice were randomly divided into seven groups of 20 mice each and injected with CNSI-DOX, DOX, CNSI or saline intraperitoneally twice at day 5 and day 9 post the inoculation of H22 cells. For CNSI-DOX and DOX groups, mice were injected with DOX equivalent dosages of 2.5 mg/kg per injection and 5 mg/kg per injection. For CNSI group, mice were injected with the CNSI equivalent dosages of CNSI-DOX groups. For saline group, mice were injected with normal saline at the same volume that was used in high dose group of CNSI-DOX. At day 13, 10 mice from each group were sacrificed and the ascites were collected for weighting. The rest 10 mice of each group were raised to day 60 for survival curve measurements.

Another set of evaluation was performed by inoculating H22 cells subcutaneously in the right flank ($2 \times 10^6$ cells per mouse). Three days later (set as day 0), when the tumors grew to an average size of 50 $mm^3$, the mice were randomly divided into four groups containing 8 mice of each. The mice were injected intraperitoneally with CNSI-DOX, DOX, CNSI and saline at 0, 3, 7, 10 and 12 d using the high dosage of aforementioned experiment (DOX equivalent dosage of 5.0 mg/kg per injection). Tumor sizes and body weights were measured three times per week. The mice were sacrificed at day 16 post the first injection. The tumors were dissected and weighted.

### 2.5. Toxicity evaluations in vivo

For toxicity evaluations, normal mice were injected with CNSI-DOX, DOX, CNSI and saline at 0, 4, 8, 11 and 15 d using the DOX equivalent dosage of 5.0 mg/kg per injection. After sacrificing at day 18 post the first injection, the blood samples were collected to prepare the serum as described in our previous report [28]. The indicators, including alanine aminotransferase (ALT), aspartate aminotransferase (AST), lactate dehydrogenase (LDH), creatine kinase (CK), creatine kinase isoenzyme MB (CK-MB) and cardiac troponin-I (cTn-I), were measured to reflect the toxicity of DOX. The heart, liver, spleen and kidneys samples were excised and fixed in 4% formalin. The samples were embedded in paraffin, sectioned using a microtome and stained by hematoxylin and eosin (H&E) for optical microscopy.

Finally, the $LD_{50}$ values of CNSI-DOX and DOX were measured. Mice were randomly divided into 14 groups containing 10 mice of each. The doses of DOX groups were 8, 10, 12.5, 15.63, 19.53 and 24.41 mg DOX/kg, respectively. The CNSI-DOX groups were injected with 10, 13.33, 17.78, 23.70, 31.60, 42.14, 56.19 and 74.92 mg DOX/kg. The numbers

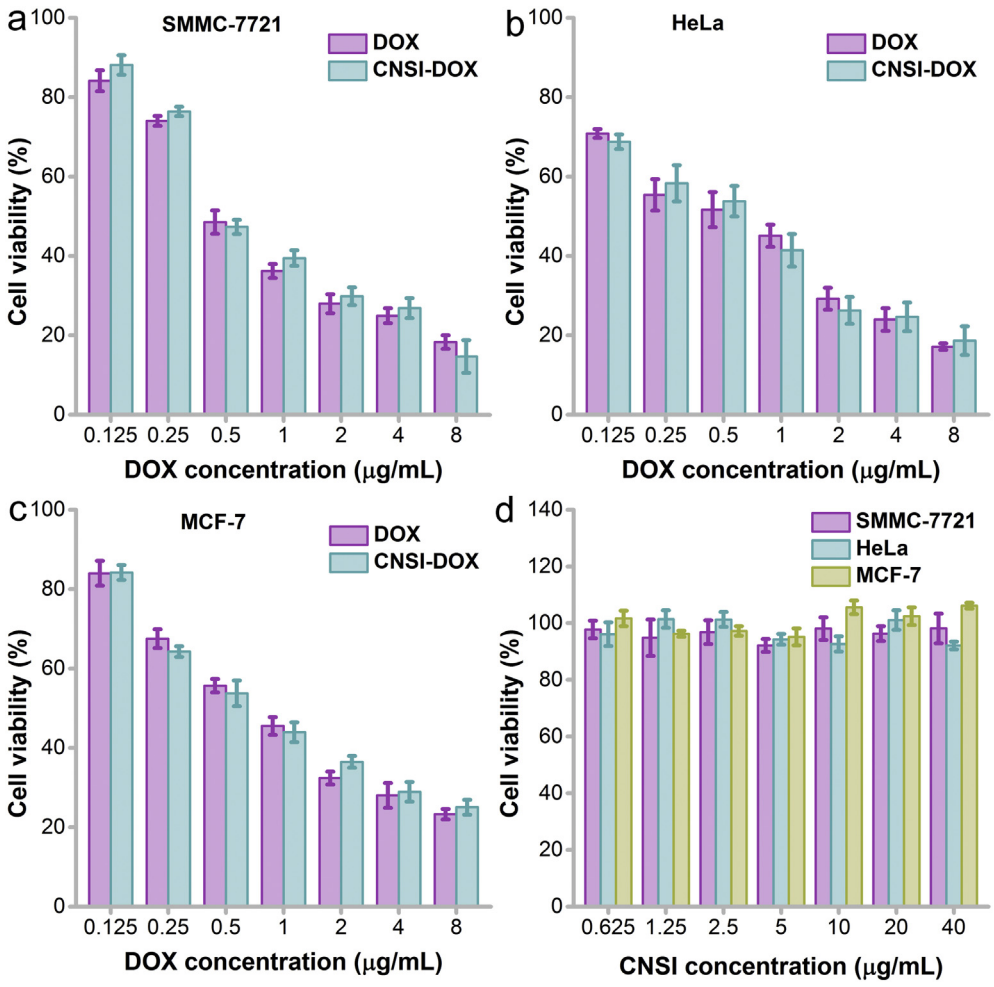


**Fig. 3.** Therapeutic effect of CNSI-DOX to cancer cells. (a) Equivalent dosage of CNSI corresponding to CNSI-DOX groups; (b) Hela cervical cancer cells; (c) SMMC-7721 liver cancer cells; (d) MCF-7 breast cancer cells.

of death for each group were recorded. The $LD_{50}$ values were calculated by the Bliss method as described in the literature [31,32].

### 2.6. Statistical analysis

All data were expressed as the mean of four individual samples with standard deviation (mean ± SD). Significance was calculated by using Student's *t*-test, where $p < 0.05$ was considered as statistically significant.

## 3. Results and discussion

### 3.1. Adsorption and release of DOX on CNSI

The characterization of CNSI was well documented in our previous papers [23,28]. The IR and XPS spectra of CNSI were provided in the Supplementary data. Generally, CNSI was formed by carbon nanoparticles wrapping by PVP. The adsorption of DOX on CNSI slightly increased the hydrodynamic radius from 191 nm to 391 nm, although the aggregates showed no change under TEM (Fig. 1), which should be due to the low contrast of DOX molecules. The adsorption induced size increase was reasonable and consistent with the literature results [17]. In addition, the adsorption was very quick. The adsorption rate reached 86.0% immediately after the mixing of CNSI and DOX (Fig. 2a). The adsorption rate was nearly saturated at 120 min (94.2%). Therefore, for clinical use, CNSI and DOX could be simply mixed before injection by mild shaking to obtain the CNSI delivered DOX. It should be noted that the pH of CNSI was 7.2 and it decreased to 6.1 after the loading of DOX. At near neutral pH, the adsorption of DOX on CNSI was efficient.

The release profile of the DOX from CNSI was shown in Fig. 2b. A pH-dependent release of DOX was observed, because DOX was ionized at lower pH and the affinity to carbon surface became weaker. The release was very quick in the first 6 h and became slower thereafter. The release rates were 69.0% at pH 2.0, 56.8% at pH 5.0 and 41.4% at pH 7.0 after 72 h dialysis. It is well known that the tumor has acidic environment [18], so CNSI-DOX would release more DOX at tumor site than at normal tissues. In addition, when CNSI-DOX enters the body, the competitive binding of proteins might further facilitate the release rate of DOX.

### 3.2. In vitro evaluation of CNSI-DOX

The inhibition of cell vitality by CNSI-DOX was evaluated on Hela cells, SMMC-7721 cells and MCF-7 cells (Fig. 3). Clearly, at higher DOX-equivalent concentration of CNSI-DOX, the cancer cell viability was inhibited more. The dose-dependent cytotoxicity of CNSI-DOX was nearly the same to that of free DOX. It could be seen that there was no significant difference between CNSI-DOX and free DOX. This was consistent with our previous report that CNSI-DOX had the same therapeutic effect to cancer cells [29]. It should be noted that CNSI alone was nontoxic to cancer cells (Fig. 3d). No viability loss was observed for the three cell lines up to CNSI concentration of 40 μg/mL. It was reported in the literature that carbon nanoparticles were of high biocompatibility to cells and animals [33,34]. Overall, our results

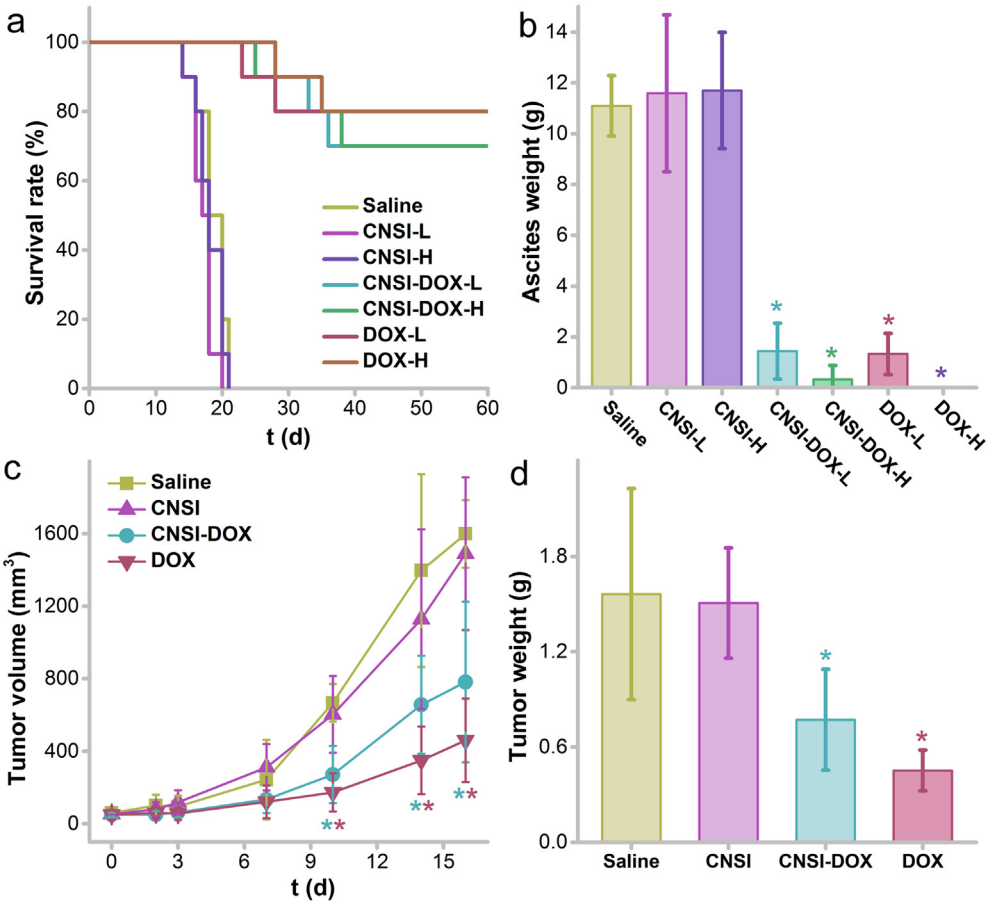


**Fig. 4.** Anti-tumor efficacy of CNSI-DOX in mice inoculated with H22 cells both intraperitoneally and subcutaneously. (a) Survival curves of ascites tumor bearing mice; (b) ascites weights; (c) tumor volumes of subcutaneous xenograft; (d) tumor weights of subcutaneous xenograft. *$p < 0.05$ compared with the saline group.

indicated that CNSI could deliver DOX to cancer cells with comparable efficacy to free DOX.

### 3.3. Antitumor efficacy of CNSI-DOX in vivo

The in vitro data suggested that CNSI-DOX had the same efficacy as free DOX, which was further confirmed in the in vivo evaluations. First, the efficacies of CNSI-DOX and free DOX were compared on ascites tumor models. As shown in Fig. 4a, CNSI had no substantial effect on the survival rate of tumor bearing mice and all of them died within three weeks. On the other hand, both CNSI-DOX and free DOX largely increased the survival rates to 90% within three weeks. The final survival rates at day 60 were 70% for CNSI-DOX groups and 80% for free DOX groups, indicating both delivered and free DOX had good therapeutic effects on ascites tumor. In another set of experiments, the mice were sacrificed at day 13 to collect the ascites for weighting. Both saline and CNSI treated groups had similar ascites weights of about 11 g, suggesting that CNSI had no therapeutic effect on ascites tumor (Fig. 4b). Statistically decrease of ascites weights were observed in CNSI-DOX and free DOX treated groups. At DOX equivalent dosage of 2.5 mg/kg, CNSI-DOX group had an ascites weight of 1.4 ± 1.1 g and the value was 1.3 ± 0.8 g for free DOX group. Increasing dosage led to lighter ascites. At DOX equivalent dosage of 5.0 mg/kg, the ascites weight of CNSI-DOX group decreased to 0.3 ± 0.6 g and no ascites could be separated for weighting in the free DOX group. There was no statistical difference between CNSI-DOX group and free DOX group at the two dosages, indicating CNSI delivery maintained the efficacy of DOX in treating ascites tumor.

Subcutaneous xenografts were also adopted to evaluate the therapeutic efficacy of the CNSI-DOX in vivo (Fig. 4c). The tumors in the control group and CNSI treated group grew rapidly in the 16-d observation period. The tumor volume of control group was 1599 ± 187 $mm^3$ at day 16. Similar volume of 1489 ± 422 $mm^3$ was observed for the CNSI treated group. The increases of tumor volume were much slower for CNSI-DOX and free DOX treated groups. The volume of tumor was 782 ± 442 $mm^3$ for CNSI-DOX group and 461 ± 230 $mm^3$ for free DOX group. The tumor volume growths of CNSI-DOX and free DOX groups were statistically lower than that of saline group after day 10. No meaningful difference was found between CNSI-DOX group and free DOX group, although the tumor volumes of CNSI-DOX groups were larger. After sacrificing, the tumor weight was measured to reflect the efficacies more accurately. As indicated in Fig. 4d, the control group (1.6 ± 0.7 g) and CNSI group (1.5 ± 0.3 g) had the highest tumor weights. Both CNSI-DOX and DOX groups showed significant inhibition on tumor weight, namely 0.8 ± 0.3 g for CNSI-DOX group and 0.5 ± 0.1 g for free DOX group. Again, no statistical difference was found between CNSI-DOX and DOX groups, but CNSI-DOX had heavier tumors. The tumor inhibition rates were calculated as 51% for CNSI-DOX group and 71% for free DOX group, indicating the high-performance of both CNSI delivered and free DOX. It should be noted that typically DOX is administrated intravenously to treat subcutaneous xenografts. However, ascites tumor bearing patients usually have metastasis, so we used intraperitoneal injection to verify the potential therapeutic effect of CNSI-DOX for metastasis during the treatment of ascites tumor preliminarily.

As described above, CNSI-DOX showed comparable performance in treating ascites tumors just as free DOX and slightly lower efficacy in treating subcutaneous xenografts. The in vitro experiments indicated the same inhibitions of cell viability by CNSI-DOX and free DOX. When CNSI-DOX reached tumor site, DOX would be released from CNSI

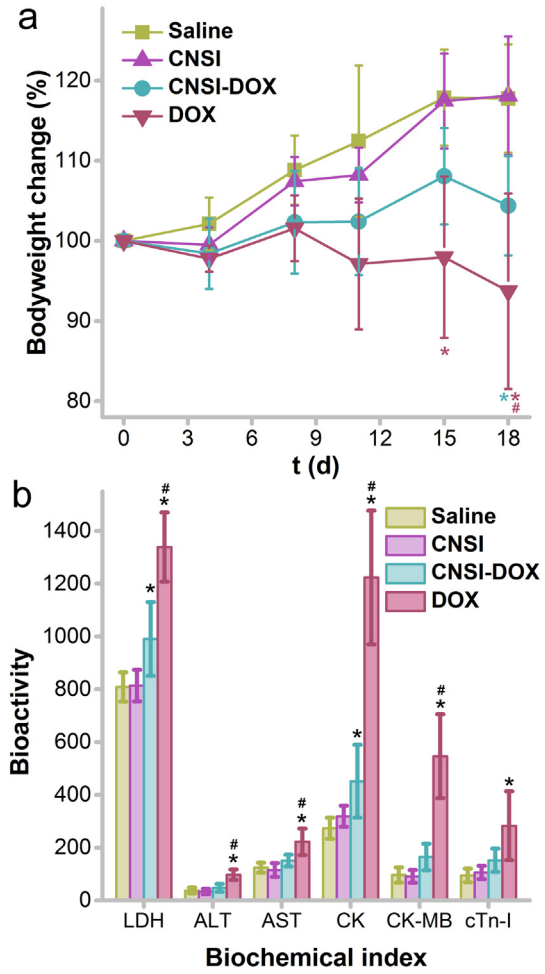


**Fig. 5.** Bodyweight increase (a) and serum biochemistry (b) of mice after the exposure to CNSI-DOX. $^{*}p < 0.05$ compared with the saline group; $^{\#}p < 0.05$ compared between CNSI-DOX group and free DOX group.

surface due to the acidic environment in tumor. Thus, for ascites tumors, the continuous release of DOX from CNSI led to the good efficacy. For subcutaneous xenografts, the translocation of DOX into blood circulation was slowed down by CNSI, which further slowed the migration of DOX to tumor via blood circulation, thus a lower efficacy was observed. Since there was no change made to CNSI itself, the clinical applications through 'off label' of CNSI are very hopeful to benefit the cancer patients in near future.

### 3.4. Toxicity of CNSI-DOX in vivo

Beyond the comparable efficacy, the main reason of using CNSI as delivery vehicle was to reduce the toxicity of free DOX. To verify this, the bodyweight, serum biochemistry and histopathology were taken as the toxicity indicators. Mice injected with CNSI showed identical bodyweight increase as the control group (Fig. 5a). The bodyweight increase of CNSI-DOX group was slower comparing to the control group. The hindered bodyweight gain became statistically lower at day 18 post-exposure. However, free DOX exposed groups had bodyweight loss rather than increase, which was quite different to the other three groups. The weight loss was statistically different to that of control group at day 15 and thereafter. It was worthwhile to note that the bodyweights were significantly different for CNSI-DOX and free DOX groups at day 18, suggesting the much lower toxicity of CNSI-DOX over the free DOX. Consistent with the bodyweight changes, the mice of free DOX group appeared to be thin and weak, resulting in 30% mortality. In contrast, the mice treated with CNSI-DOX behaved normally with a much lower mortality (10%).

Serum biochemical parameters are more sensitive than the bodyweight change. Here, we measured the serum levels of ALT, AST, LDH, CK, CK-MB and cTn-I to reflect the toxicity of CNSI-DOX to liver and heart (Fig. 5b). Here, LDH is an indicator for the liver and heart damage. ALT and AST are sensitive indicators for the hepatic function damage. CK and CK-MB are cardiac enzymes that indicate the heart function. cTn-I is a sensitive and specific parameter for heart function damage. Again, free DOX showed the highest toxicity to mice that all parameters showed significant increases comparing to those of the control group. Upon the deliver by CNSI, only CK level showed significant increase, but the CK level of CNSI-DOX group was about 1/3 of that of free DOX group. The increased CK levels suggested the toxicity of CNSI-DOX to heart was lower than free DOX. Another issue to notice was that free DOX group had statistically higher serum biological parameters than CNSI-DOX group except cTn-l. This confirmed that CNSI largely alleviated the toxicity of free DOX to liver and heart.

No significant histopathological change was found in the heart, liver, spleen and kidneys of the mice treated with CNSI and CNSI-DOX, either (Fig. 6). CNSI-DOX group had nearly the same histopathology as the control group, indicating the low toxicity of CNSI-DOX to mice. In contrast, serious histopathological changes were induced by free DOX in these organs. Mild edema, gap increase and fracture of myocardial fiber were observed in heart. Mild edema and necrosis of liver cells were presented. Some of the hepatic cells became irregular in shape and more vacuoles formed. The spleen nodules atrophy, irregular shape, blurred boundaries, altered rate of red pulp and white pulp were found in the spleen section. Glomerular capillary congestion and expansion were observed in kidneys. The edema of renal tubular epithelial cell and irregular vacuoles were also found in kidneys. The aforementioned histopathological changes were consistent with the serum biochemistry that free DOX were more toxic than CNSI delivered DOX. Overall, CNSI alleviated the histopathological changes of DOX in heart, liver, spleen and kidneys.

Another direct toxicity comparison between CNSI-DOX and free DOX was made by measuring the $LD_{50}$ values. The free DOX had a $LD_{50}$ of 15.2 mg/kg (95% confidence interval: 13.9–16.6 mg/kg), which was consistent with the literature results (20 mg/kg) [35]. The $LD_{50}$ of CNSI-DOX was 43.8 mg/kg (95% confidence interval: 38.2–50.2 mg/kg), nearly three times of that of free DOX. The increased $LD_{50}$ indicated that CNSI reduced the acute toxicity of DOX to mice. In our study, the mice received the high dosage of 5 mg/kg, much lower than the $LD_{50}$. For CNSI-DOX, the larger $LD_{50}$ might allow higher dosage when needed, while free DOX could not adopt higher dosage.

Our results collectively indicated that CNSI could largely reduce the toxicity of DOX while maintaining its efficacy. A possible explanation of the reduced toxicity of free DOX upon CNSI delivery could be the slower release of DOX at neutral pH (Fig. 2b). Previous studies have demonstrated that CNSI could decrease the blood concentration of DOX [29], which consequently might reduce its toxicity. Many other studies using diverse delivery vehicles also confirmed that the controlled release of DOX could alleviate its toxicity in vivo [11–14]. It should be noted that CNSI itself was nontoxic to mice in our study and other evaluations [29,30]. The clinical applications on over 100,000 patients per year also supported the biosafety of using CNSI for biomedical purpose. The advantages of reduced toxicity were obvious, including the fewer hazards to the weak patients and the accessible higher dosage to overcome the drug residence.

## 4. Conclusions

In summary, CNSI retained the therapeutic efficacy and largely reduced the toxicity of DOX, where the $LD_{50}$ value of CNSI delivered DOX was nearly two times higher than that of free DOX. Similar antitumor efficacies of CNSI delivered and free DOX were observed in vitro. CNSI

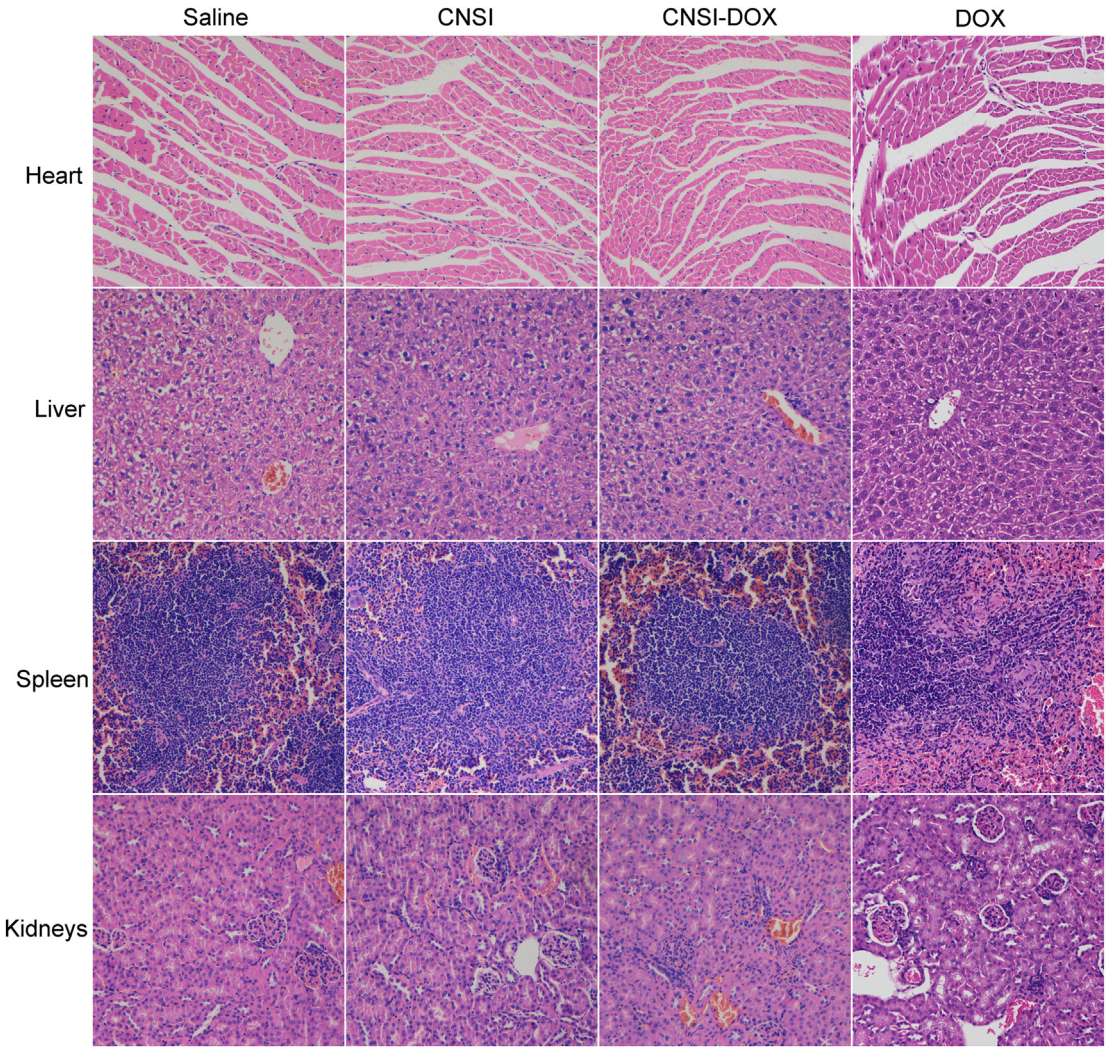


**Fig. 6.** Histological morphology changes of heart, liver, spleen, and kidneys after the exposure to CNSI-DOX.

delivered DOX also showed as good inhibitory effects as free DOX on both hepatoma ascites tumor and subcutaneous tumor, while the former (CNSI-DOX) had much lower toxicity. Taking the good biocompatibility of CNSI in consideration, our results here presented a new application of CNSI in chemotherapy and extended the applications of CNSI from sole lymph node mapping toward theranostics. Clinical applications through 'off label' use should be urgently evaluated to benefit the cancer patients. It is hoped that our results would stimulate more clinical applications of CNSI in theranostics and benefit the development of nanomaterials for biomedical applications [36–41].

## Conflicts of interest

Y. Huang, X. Zhang, G. Zeng, Q. Xin and X.-H. Tang are employees of Chongqing Lummy Pharmaceutical Co. Ltd. The authors report no other conflicts of interest in this work.

## Acknowledgements

We acknowledge financial support from the major drug discovery science and technology major projects of 12th five-year national plan and research fund for major drug research of Nation Science and Technology (863 Projects, 2012ZX09102001-4 and 2012ZX09102101-015) and the National Program for Support of Top-notch Young Professionals, Southwest Minzu University (No. 2016NZDFH01) and the Fundamental Research Funds for the Central Universities.

## Appendix A. Supplementary data

Supplementary data to this article can be found online at https://doi.org/10.1016/j.msec.2018.07.012.

## References

[1] C. Carvalho, R.X. Santos, S. Cardoso, S. Correia, P.J. Oliveira, M.S. Santos, P.I. Moreira, Curr. Med. Chem. 16 (2009) 3267–3285.
[2] V. Hanusova, I. Bousova, L. Skalova, Drug Metab. Rev. 43 (2011) 540–557.
[3] K. Chatterjee, J. Zhang, N. Honbo, J.S. Karliner, Cardiology 115 (2010) 155–162.
[4] G. Takemura, H. Fujiwara, Prog. Cardiovasc. Dis. 49 (2007) 330–352.
[5] Y. Octavia, C.G. Tocchetti, K.L. Gabrielson, S. Janssens, H.J. Crijns, A.L. Moens, J. Mol. Cell. Cardiol. 52 (2012) 1213–1225.
[6] S. Alpsoy, C. Aktas, R. Uygur, B. Topcu, M. Kanter, M. Erboga, O. Karakaya, A. Gedikbasi, J. Appl. Toxicol. 33 (2013) 202–208.
[7] R. Panchuk, N. Skorokhyd, V. Chumak, L. Lehka, S. Omelyanchik, V. Gurinovich, A. Moiseenok, P. Heffeter, W. Berger, R. Stoika, Croat. Med. J. 55 (2014) 206–217.
[8] O. Chiuzbaian, M. Gharanei, C.J. Mee, H. Maddock, E. Hatch, J. Pharmacol. Toxicol. Methods 88 (2017) 216.
[9] M. Cagel, E. Grotz, E. Bernabeu, M.A. Moretton, D.A. Chiappetta, Drug Discov. Today 22 (2017) 270–281.
[10] Q. Chen, M. Long, L. Qiu, M. Zhu, Z. Li, M. Qiao, H. Hu, X. Zhao, D. Chen, Int. J. Nanomedicine 11 (2016) 5415–5427.
[11] M. Fojtu, J. Gumulec, T. Stracina, M. Raudenska, A. Skotakova, M. Vaculovicova, V. Adam, P. Babula, M. Novakova, M. Masarik, Curr. Drug Metab. 18 (2017) 237–263.
[12] D. Matyszewska, Surf. Innov. 2 (2014) 201–210.

[13] J.G. Reynolds, E. Geretti, B.S. Hendriks, H. Lee, S.C. Leonard, S.G. Klinz, C.O. Noble, P.B. Lücker, P.W. Zandstra, D.C. Drummond, K.J. Olivier Jr., U.B. Nielsen, C. Niyikiza, S.V. Agresta, T.J. Wickham, Toxicol. Appl. Pharmacol. 262 (2012) 1–10.
[14] C. Sun, L. Zhou, M. Gou, S. Shi, T. Li, J. Lang, Oncol. Rep. 35 (2016) 3600–3606.
[15] I.Y. Zhitnyak, I.N. Bychkov, I.V. Sukhorukova, A.M. Kovalskii, K.L. Firestein, D. Golberg, N.A. Gloushankova, D.V. Shtansky, ACS Appl. Mater. Interfaces 9 (2017) 32498–32508.
[16] M. Seke, D. Petrovic, A. Djordjevic, D. Jovic, M.L. Borovic, Z. Kanacki, M. Jankovic, Nanotechnology 27 (2016) 485101.
[17] Y. Wang, S.T. Yang, Y. Wang, Y. Liu, H. Wang, Colloids Surf. B 97 (2012) 62–69.
[18] Z. Liu, A.C. Fan, K. Rakhra, S. Sherlock, A. Goodwin, X. Chen, Q. Yang, D.W. Felsher, H. Dai, Angew. Chem. Int. Ed. Eng. 48 (2009) 7668–7672.
[19] F. Wang, Q. Sun, B. Feng, Z. Xu, J. Zhang, J. Xu, L. Lu, H. Yu, M. Wang, Y. Li, W. Zhang, Adv. Healthc. Mater. 5 (2016) 2227–2236.
[20] X. Zhang, Y. Wang, W. Liu, X. Liang, B. Si, E. Liu, X. Hu, J. Fan, Mater. Lett. 209 (2017) 360–364.
[21] D. Wang, C. Hou, L. Meng, J. Long, J. Jing, D. Dang, Z. Fei, P.J. Dyson, J. Mater. Chem. B 5 (2017) 1380–1387.
[22] Y. He, L. Zhang, Z. Chen, Y. Liang, Y. Zhang, Y. Bai, J. Zhang, Y. Li, J. Mater. Chem. B 3 (2015) 6462–6472.
[23] P. Xie, Q. Xin, S.T. Yang, T. He, Y. Huang, G. Zeng, M. Ran, X. Tang, Int. J. Nanomedicine 12 (2017) 4891–4899.
[24] Z. Li, S. Ao, Z. Bu, A. Wu, X. Wu, F. Shan, X. Ji, Y. Zhang, Z. Xing, J. Ji, World J. Surg. Oncol. 14 (2016) 88.
[25] X. Wu, Q. Lin, G. Chen, J. Lu, Y. Zeng, X. Chen, J. Yan, PLoS One 10 (2015) e0135714.
[26] Y. Zhu, X. Chen, H. Zhang, L. Chen, S. Zhou, K. Wu, Z. Wang, L. Kong, H. Zhuang, Head Neck 88 (2016) 840–845.
[27] J. Gu, J. Wang, X. Nie, W. Wang, J. Shang, Int. J. Clin. Exp. Med. 8 (2015) 9640–9648.
[28] P. Xie, S.T. Yang, T. He, S. Yang, X.H. Tang, Int. J. Mol. Sci. 18 (2017) E2562.
[29] P. Xie, X. Tang, L. Li, Z. Qian, M. Ran, X. Zhang, Q. Xin, H. Luo, J. Nanosci. Nanotechnol. 16 (2016) 6910–6918.
[30] Q. Yang, X.D. Wang, J. Chen, C.X. Tian, H.J. Li, Y.J. Chen, Q. Lv, Tumor Biol. 33 (2012) 2341–2348.
[31] G. Yuan, S. Dai, Z. Yin, H. Lu, R. Jia, J. Xu, X. Song, L. Li, Y. Shu, X. Zhao, Food Chem. Toxicol. 65 (2014) 260–268.
[32] C. Zhang, Y. Yi, J. Chen, R. Xin, Z. Yang, Z. Guo, J. Liang, R. Shang, Molecules 20 (2015) 5299–5312.
[33] J.H. Liu, S.T. Yang, X. Wang, H. Wang, Y. Liu, P.G. Luo, Y. Liu, Y.P. Sun, ACS Appl. Mater. Interfaces 6 (2014) 14672–14678.
[34] S.T. Yang, X. Wang, H. Wang, F. Lu, P.G. Luo, L. Cao, M.J. Meziani, J.H. Liu, Y. Liu, M. Chen, Y. Huang, Y.P. Sun, J. Phys. Chem. C 113 (2009) 18110–18114.
[35] M.M. Joseph, S.R. Aravind, S.K. George, K.R. Pillai, S. Mini, T.T. Sreelekha, J. Biomed. Nanotechnol. 10 (2014) 3253–3268.
[36] X. Zhang, S. Wang, L. Xu, L. Feng, Y. Ji, L. Tao, S. Li, Y. Wei, Nano 4 (2012) 5581–5584.
[37] X. Zhang, K. Wang, M. Liu, X. Zhang, L. Tao, Y. Chen, Y. Wei, Nano 7 (2015) 11486–11508.
[38] Y. Shi, R. Jiang, M. Liu, L. Fu, G. Zeng, Q. Wan, L. Mao, F. Deng, X. Zhang, Y. Wei, Mater. Sci. Eng. C 77 (2017) 972–977.
[39] G. Zeng, M. Liu, R. Jiang, C. Heng, Q. Huang, L. Mao, J. Hui, F. Deng, X. Zhang, Y. Wei, Mater. Sci. Eng. C 77 (2017) 420–426.
[40] L. Huang, M. Liu, L. Mao, X. Zhang, D. Xu, Q. Wan, Q. Huang, Y. Shi, F. Deng, X. Zhang, Y. Wei, Mater. Sci. Eng. C 76 (2017) 586–592.
[41] Z. Long, M. Liu, L. Mao, G. Zeng, Q. Huang, H. Huang, F. Deng, Y. Wan, X. Zhang, Y. Wei, Mater. Sci. Eng. C 73 (2017) 252–256.